

Fabrication of Theta Carbon Nanopipettes using a Template-Based Chemical Vapor Deposition Nanomanufacturing Process

Ayomipo Arowosola¹, Akane Fujimoto², Olivia Scheibel³, and Michael G. Schrlau^{3*}

¹Department of Materials Science and Engineering, Rochester Institute of Technology, Rochester, NY, USA

²Department of Industrial & Systems Engineering, Rochester Institute of Technology, Rochester, NY, USA

³Department of Mechanical Engineering, Rochester Institute of Technology, Rochester, NY, USA

*Corresponding Author: mgseme@rit.edu

Abstract—In recent years, there has been much effort towards creating carbon nanopipettes and endoscopes to probe single living cells. These devices, consisting of a single carbon nanotube attached to the end of a pulled glass capillary, have been utilized successfully as single cell injectors, electrodes, and sensors. In this work, we report the fabrication of a carbon nanopipette with two independent carbon nanostructures at its tip using a template-based chemical vapor deposition (TB-CVD) nanomanufacturing process. Here, carbon film was selectively deposited on the lumen walls of a pulled theta glass capillary to form two independent carbon channels throughout the entire capillary; subsequent wet-etching of the glass at the tip exposed two carbon nanostructures. The resultant probe consists of two hollow and conductive carbon nanostructures at the tip of the pulled capillary, where their shape and dimensions are controlled by process parameters. Using standard cell physiology equipment, we show the probe is capable of fluid transport via dye ejection from the tip. The work herein demonstrates how integrative nanomanufacturing processes can be used to fabricate probes with multiple independent carbon nanostructures within a small footprint for potential single cell applications.

Keywords—*Nanomanufacturing; Chemical Vapor Deposition; Carbon Nanopipette; Fluid Transport*

I. INTRODUCTION

Cancer and heart related deaths account for approximately 50% of all occurring deaths in the United States. This fact has held true through several years [1]. The impact of this in the United States has led to many research focused on the causes and aggravation of these diseases [2-8]. These research efforts predominantly involve cell physiology – the biological studies of different cells, their mechanisms, and interactions with their surrounding environment. Glass micropipettes are among the most widely used tools for cell physiology, with tip diameters ranging from hundreds of nanometers to a few micrometers in size [9]. Compared to single cells with diameters in the tens of micrometers, glass micropipettes are

relatively large and can cause irreparable damage to cells, leading to cell necrosis. The need for functional tools that facilitate single cell analysis has resulted in the fabrication of minimally invasive nanoscale tools for intracellular applications, such as intracellular injection and biosensing [10-19].

In previous work, we reported the development of carbon nanopipettes (CNPs); a single carbon nanotube (CNT) integrated into the tip of a pulled glass capillary without assembly using template-based chemical vapor deposition (TB-CVD) processes [16]. Briefly, carbon was deposited in the inner lumen of a pulled quartz capillary (micropipette) via chemical vapor deposition (CVD) to form a CNT inside the micropipette tip. The CNT was then exposed by wet-etching the quartz at the tip of the micropipette. CNPs were hollow and conductive from the tip to the distal end, allowing minimally invasive intracellular injection and cell electrophysiology [16]. However, these probes consisted of a single nanotube at their tip, limiting the functions that could be performed while inside the cell.

In this work, we report the fabrication of theta carbon nanopipettes (TCNPs), which have two carbon nanostructures integrated into the tip of a pulled theta glass capillary (Fig. 1). Template-based nanomanufacturing processes, modified from those developed previously [16], were employed to manufacture TCNPs in three steps without assembly: (i) forming templates by pulling micropipettes from theta glass capillaries; (ii) selectively depositing carbon via CVD on the lumen walls of the micropipette; and (iii) exposing the two carbon nanostructures formed at the micropipette tip with selective wet-etching. Here, pulling parameters control the geometry of the nanostructure, CVD time and temperature control the thickness of the nanostructure wall, and wet etching rate controls the length of exposed nanostructure. The resultant probe consists of two distinct carbon nanostructures within a submicron-diameter tip, each independently hollow and conductive from the tip to the distal end.

II. FABRICATION

As shown in Fig. 1a, TCNPs were manufactured in three steps – pipette pulling, carbon deposition and etching. The resultant probes consisted of two

independent carbon nanostructures integrated into a pulled capillary (Fig. 1b); probes with nanoscopic tips

can be manufactured using this process (Fig. 1c).

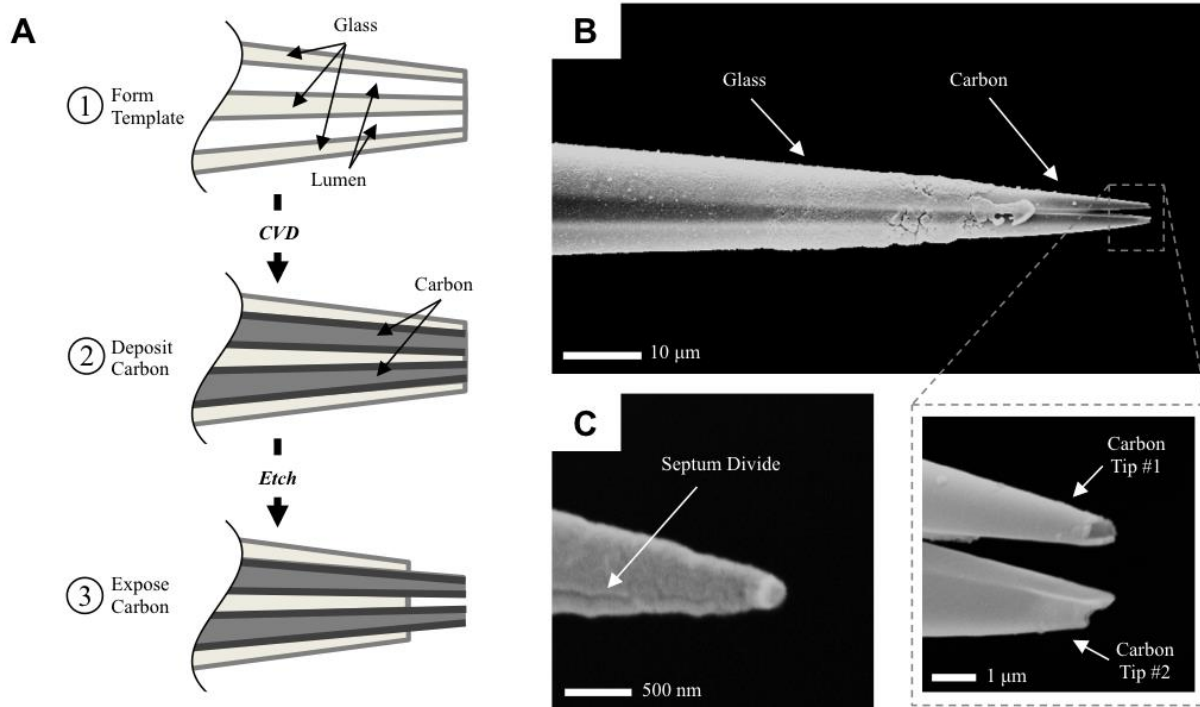


Fig. 1: A) Schematic of the TCNP fabrication. B) SEM micrograph of TCNP showing the presence of two carbon tips (boxed region). C) SEM micrograph showing two tips terminating at a nanoscale tip.

A. Pipette Pulling

Quartz capillaries with two independent, separate channels were pulled with a pipette puller (P2000F, Sutter Instrument). The pipette puller has 5 governing pulling parameters – *Heat*, *Filament*, *Delay*, *Velocity* and *Pull*, which all have to be specified in manufacturer-designated arbitrary units (au) to form a specific pulling program. These programs eventually determine the overall geometry of the pulled pipettes.

In this work, two pulling studies were designed and carried out to determine how the micropipette tip

diameter and taper length were affected as a function of pulling parameters. One study involved varying the *Heat* parameter, while other parameters are unchanged (referred to herein as *H-programs*); the other involved varying the *Pull* parameter, while other parameters remain unchanged (referred to herein as *P-programs*). The experimental matrix and sample identification for these two studies of *H-programs* (H1 to H7) and *P-programs* (P1 to P5) are reported in Table 1. For odd *H-programs*, the sample size per programs, $n = 6$; For even *H-programs* and all *P-programs*, $n = 4$.

Table 1: Pipette Pulling Experiments and Results

Sample	Pulling Parameters					Taper Length ± SD (mm)	Taper Diameter ± SD (μm)
	H	F	V	D	P		
H1	700	5	40	130	150	5.0 ± 0.4	1.0 ± 0.0
H2	750	5	40	130	150	8.0 ± 0.0	0.8 ± 0.1
H3	800	5	40	130	150	10.0 ± 1.1	0.9 ± 0.1
H4	850	5	40	130	150	12.5 ± 0.6	0.7 ± 0.0
H5	900	5	40	130	150	14.0 ± 0.5	0.8 ± 0.0
H6	950	5	40	130	150	15.0 ± 0.5	0.5 ± 0.0
H7	999	5	40	130	150	17.0 ± 0.6	0.6 ± 0.1
P1	900	5	40	130	50	-	-
P2	900	5	40	130	100	7.2 ± 0.4	0.9 ± 0.1
P3	900	5	40	130	150	11.9 ± 0.8	0.6 ± 0.1
P4	900	5	40	130	200	13.9 ± 0.2	0.5 ± 0.1
P5	900	5	40	130	255	14.4 ± 0.4	0.5 ± 0.0
TL1	700	10	50	150	60	3.1 ± 0.5	1.3 ± 0.3
	750	15	40	140	135		

The diameter of the pulled pipette tip and the pulled taper length (distance from the tip to the beginning of the taper) as a function of *Heat* and *Pull* parameters were measured from optical images. The average and standard deviations of the taper length and tip diameter were then calculated (Table 1). As shown in Table 1, pipettes made from theta glass could be pulled with a single line program to achieve micro- and sub-micrometer outer diameters (0.5 – 1.0 μm) over a wide range of taper lengths (5.0 – 17.0 mm). However, two line pulling programs were able to achieve the shortest taper lengths (3.1 mm).

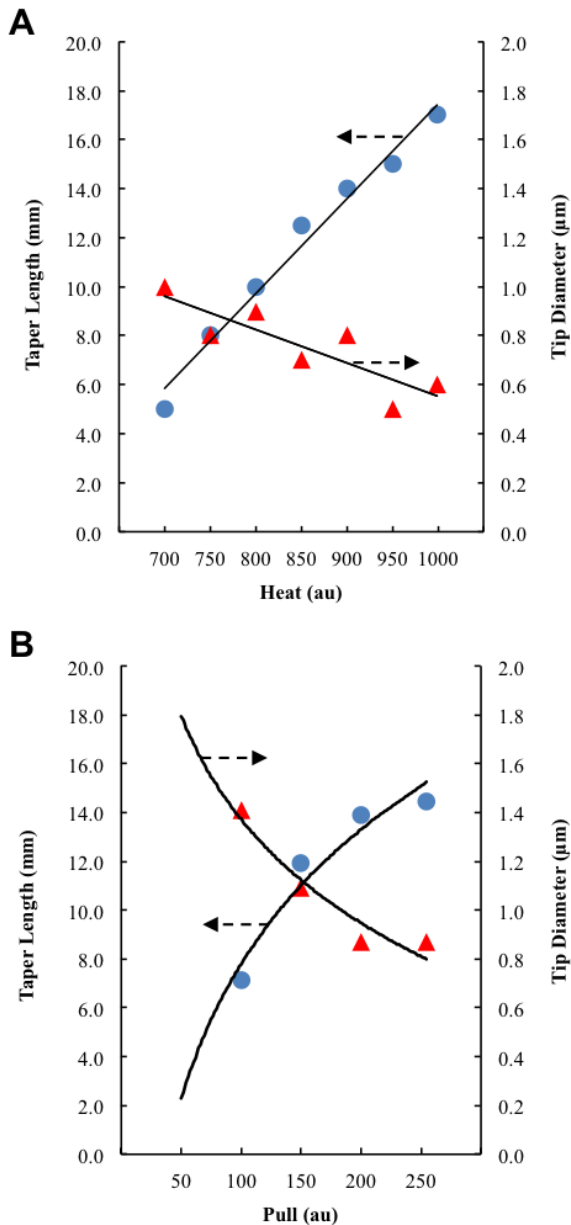


Fig. 2: Taper length and tip diameter dependence on A) Heat and B) Pull.

The average and standard deviations of the taper length and tip diameter were plotted as a function of *Heat* and *Pull* parameters (Fig. 2). As shown in Fig. 2a, taper length increased as *Heat* increased. However, tip diameter decreased as *Heat* increased. For example, pulling a pipette with a short taper length

of 5.0 mm results in a larger tip diameter of 1.0 μm (Sample H1), while pulling a pipette with a long taper length of 15 mm results in a pipette with a small tip diameter of 0.5 μm (Sample H6). A similar effect occurs as a function of *Pull*, as shown in Fig. 2b. In other words, as *Pull* increased, taper length increased but tip diameter decreased. These results highlight the general trade-off between taper length and tip diameter of a pulled glass micropipette [20].

B. Carbon Deposition

Carbon was deposited on the inner lumens of the pulled pipettes via CVD using Methane as the carrier gas and Argon as the precursor gas. CVD was carried out with an Argon flow rate of 300 sccm and Methane flow rate of 200 sccm for various deposition times and temperatures. Changes in deposition time and temperature resulted in different thicknesses of deposited carbon, as described in literature [21]. Fig. 3 shows a typical SEM image of a fractured pipette, where the deposition of carbon on the inner lumen of quartz can be visualized.

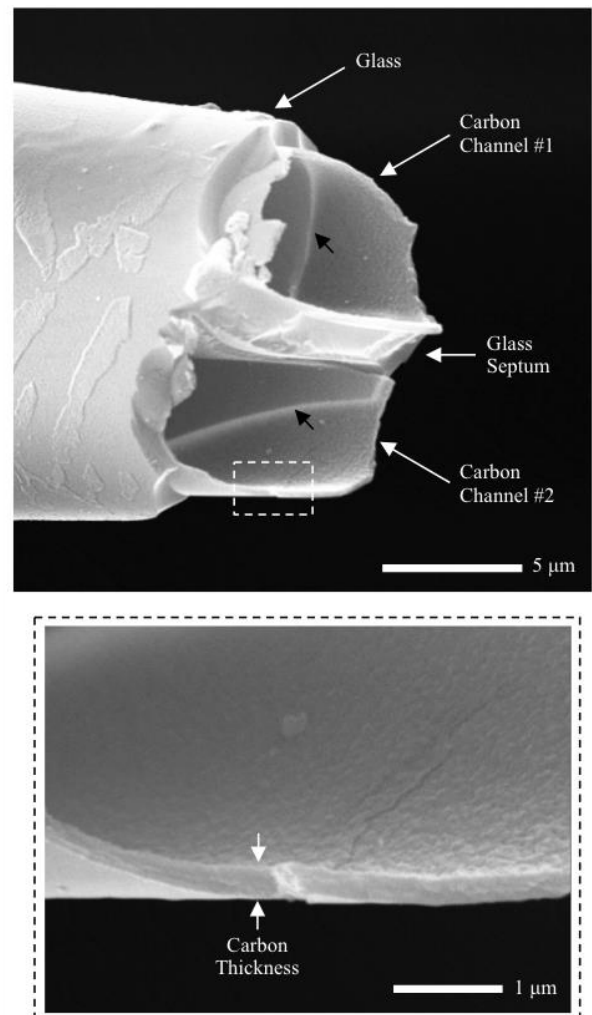


Fig. 3: SEM micrographs of a broken TCNP showing the carbon channels formed within the pulled theta glass capillary. The glass can be seen through the electron-transparent carbon film (black arrows). Higher magnification micrographs show the thickness of the carbon film (boxed region).

The effect of varying deposition time was observed in the TCNPs, where a longer deposition time resulted in a larger carbon film thickness. To this end, the tips of TCNPs, manufactured at 950°C for 1 hr and 2 hrs, were fractured to produce cross section outer diameters of approximately 17 μm . We measured carbon film thicknesses of approximately 380 nm and 400 nm for TCNPs manufactured for 1 and 2 hours, respectively. Thickness also increased as a function of deposition temperature. Here, TCNPs were manufactured for 30 min and fractured at 11 μm diameter. From SEM micrographs, the measured carbon thickness was 140 nm and 260 nm at a carbon deposition temperature of 920°C and 930°C, respectively.

Measurements from SEM micrographs suggest the thickness of the carbon film decreases axially, moving away from the TCNP tip. Here, TCNPs were manufactured at a CVD temperature of 930°C and carbon deposition time of 15 minutes. TCNPs were fractured at two different lengths to produce cross section outer diameters of approximately 34 μm and 110 μm . The carbon thickness at the tip and at 34 μm and 110 μm outer diameters were 220 nm, 180 nm and 150 nm, respectively. This trend is also observed in TCNPs manufactured at 930°C, 30 min and at 950°C, 1 hr.

C. Etching

The TCNPs were etched in 10:1 buffered hydrofluoric acid (BHF) at room temperature for 2, 5, 8, 10 and 15 minutes, and the exposed carbon tip lengths were measured using an optical microscope. As seen in Fig. 4, a longer etch time exposes more carbon. Also, H1 and TL1 were compared and we observed a downward shift in the generated curves from H1 to TL1. This shift implies that for the same etch time, a shorter carbon length is exposed in TL1 than H1. This further confirms that the taper geometry of TL1 is in fact quite different from that of H1 as observed by optical microscopy.

Since BHF etches TCNPs at the same rate, it would remove the same amount of glass, in the same time, on both types of pipettes. The difference in exposed carbon length is explained in the amount of glass present at the tips of the TCNPs. The TL1 pipettes produced blunter tapers compared with the H1 pipettes and thus have more glass at the tip/taper. This difference is also observed in the optical images of pipettes pulled with these two programs.

III. FLUID TRANSPORT THROUGH TCNPs

To facilitate fluid transport through the sub-micrometer tip of the TCNP, a short taper length is desired to reduce friction between the fluid and the pipette and ultimately reduce resistance to flow, driven by pressure injection [22]. This fact, together with earlier results that showed a trade-off between these two properties compelled us to try other variations of pulling parameters to achieve a desired geometry that works for intracellular fluid injection. In an attempt to

pull a short taper length pipette, and based on the general pipette pulling trend discussed above, different variations of programs were tried. Results found that a 2-line program (Sample TL1; $n = 9$) produced desirable results, as also shown in Table 1.

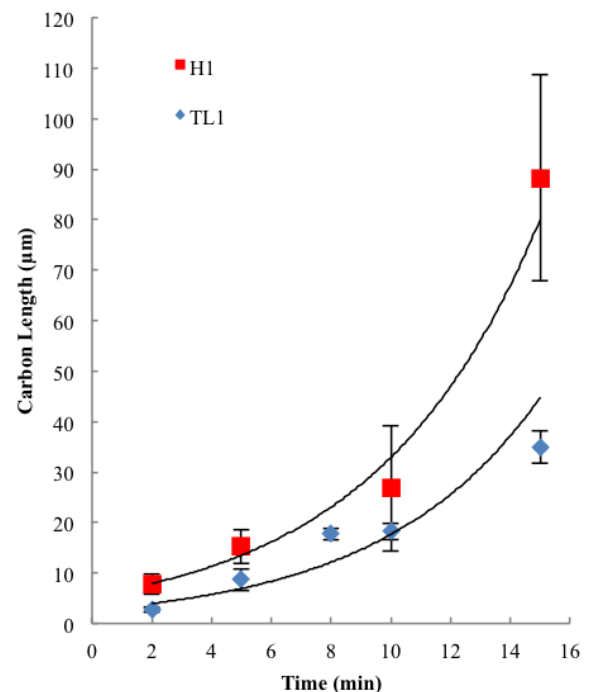


Fig. 4: Comparison between H and TL programs of exposed carbon length as a function of etching time.

Comparing to pipettes produced with single line pulling programs (H1-7, P1-5), pipettes produced with two line pulling programs (TL1) consisted of tip diameters of approximately 1 μm and the shortest taper length (3 mm). Furthermore, an analysis of optical images of both H and TL programs show a difference in the rate of diameter change per unit length as we move away from the tip of the pipette. In the *H-program* pipette, the rate of change was observed to remain constant over a length of approximately 260 μm , while over the same length, a 50% increase in rate of change was observed in the *TL-program*. This drastic increase in rate of change of diameter per unit length shows that pipettes pulled with the *TL-program* exhibit a wider girth than those pulled with the *H-program* as we move away from the pipette tip. This reduces resistance to fluid flow in TL pipettes and facilitates fluid transport.

Fluid transport studies were carried out utilizing a commercially available pressure injection system. To this end, fluorescent dye (15 μM Dextran, tetramethylrhodamine, Invitrogen™) was filtered with a 20 nm pore size inorganic membrane filter (Anotop 10 Plus, Whatman™) and backfilled into the two channels of a TCNP (Sample TL1). The TCNP was tapped several times to remove any air bubbles within the taper length of the probe. The fluid-prepared TCNP was then connected to the injection system (FemtoJet, Eppendorf™) and lowered into a clear bottom dish of de-ionized (DI) water with a

commercially available micromanipulator (TransferMan NK2, Eppendorf™). All fluid transport experiments were conducted under an inverted fluorescence microscope (AxioObserver.A1m, Zeiss) to observe the ejection of fluorescent dye from the TCNP tip.

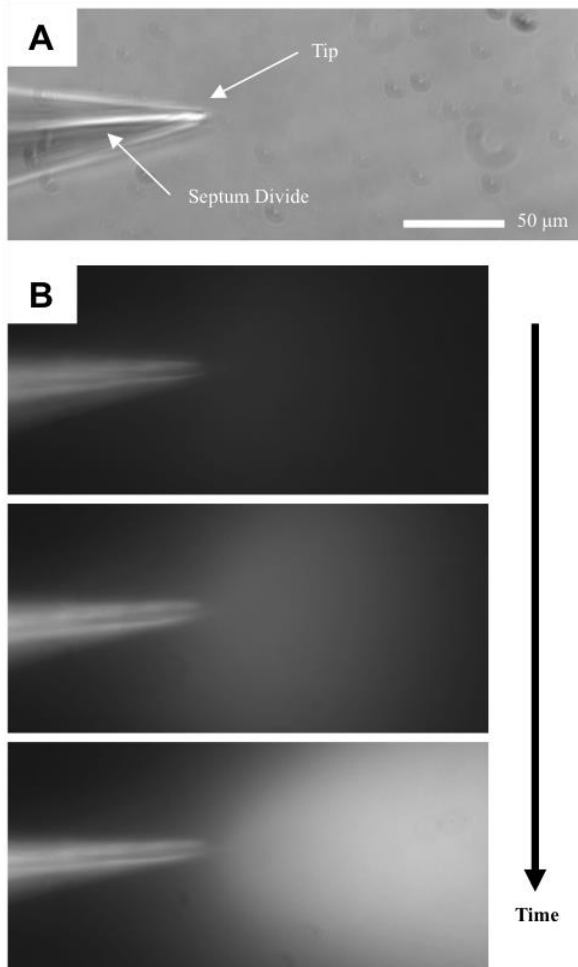


Fig. 5: A) Optical image of TCNP in DI water. B) Chronological occurrence of an injection trial.

As shown in Fig. 5A, the tip of the TCNP and the division between the two channels can be observed in brightfield under the optical microscope. Upon

[1]D. L. Hoyert, "75 years of mortality in the United States, 1935–2010 NCHS data brief," ed. Hyattsville, MD: National Center for Health Statistics, 2012.

[2]A. Valavanidis, T. Vlachogianni, and K. Fiotakis, "Tobacco smoke: involvement of reactive oxygen species and stable free radicals in mechanisms of oxidative damage, carcinogenesis and synergistic effects with other respirable particles," *International Journal of Environmental Research and Public Health*, 6:445-462, 2009.

[3]P. Pacher, J. S. Beckman, and L. Liaudet, "Nitric oxide and peroxynitrite in health and disease," *Physiological Reviews*, 87:315-424, 2007.

[4]T. Chang and L. Wu, "Methylglyoxal, oxidative stress, and hypertension," *Canadian Journal of Physiology and Pharmacology*, 84:1229-1238, 2006.

applying a constant backend pressure of 150 hPa to the fluid-filled TCNP, fluorescent dye was ejected from the micrometer-sized tip. As shown in Fig. 5B, fluorescent dye continued to be ejected as long as the pressure was applied, resulting in an increased fluorescent intensity at the end of the TCNP tip over time. These results demonstrate that it is possible to manufacture probes consisting of multiple hollow independent carbon nanostructures within a micrometer-sized tip.

IV. CONCLUSION

In this work, we reported the methodology for fabricating a carbon nanopipette with two independent carbon nanostructures integrated into its tip using a three-step template-based nanomanufacturing technique. The shape and dimensions of the nanostructures can be controlled by process parameters. Using standard cell physiology equipment, we showed the probe is capable of fluid transport via dye ejection from the tip. The work herein demonstrates how integrative nanomanufacturing processes can be used to fabricate probes with multiple independent carbon nanostructures within a small footprint for potential single cell applications.

ACKNOWLEDGMENTS

The authors acknowledge funding from the Texas Instruments / Douglas Harvey 2012 Faculty Award. MS and AA acknowledge the financial gift for student support from Professor Emeritus Balwant Karlekar and his wife, Lata. AA acknowledges financial support from the RIT School of Chemistry and Materials Science and the continued support of Ms. Brenda Mastrangelo. AF acknowledges financial support from the RIT Honors Program. The authors acknowledge Dr. Richard Hailstone from the RIT Nanomaging Laboratory and Mr. Masoud Golshadi for SEM imaging and technical support.

REFERENCES

[5]D. Jay, H. Hitomi, and K. K. Griendling, "Oxidative stress and diabetic cardiovascular complications," *Free Radical Biology and Medicine*, 40:183-192, 2006.

[6]C. Bogdan, "Nitric oxide and the immune response," *Nature Immunology*, 2:907-916, 2001.

[7]D. A. Wink, Y. Vodovotz, J. Laval, F. Laval, M. W. Dewhirst, and J. B. Mitchell, "The multifaceted roles of nitric oxide in cancer," *Carcinogenesis*, 19:711-721, 1998.

[8]H. Wiseman and B. Halliwell, "Damage to DNA by reactive oxygen and nitrogen species: role in inflammatory disease and progression to cancer," *The Biochemical Journal*, 313:17-29, 1996.

[9]H. Matsuoka and M. Saito, "High throughput microinjection technology toward single-cell bioelectrochemistry," *Electrochemistry*, 74:12-18, 2006.

[10]C. Y. Li, X. Z. Xu, and D. Tigwell, "A simple and comprehensive method for the construction, repair and recycling of single and double tungsten microelectrodes," *Journal of Neuroscience Methods*, 57:217-220, 1995.

[11]W. Pak Kin, U. Ulmanella, and H. Chih-Ming, "Fabrication process of microsurgical tools for single-cell trapping and intracytoplasmic injection," *Journal of Microelectromechanical Systems*, 13:940-946, 2004.

[12]K. Yum, H. N. Cho, J. Hu, and M.-F. Yu, "Individual nanotube-based needle nanoprobe for electrochemical studies in picoliter microenvironments," *ACS Nano*, 1:440-448, 2007.

[13]R. Singhal, Z. Orynbayeva, R. V. K. Sundaram, J. J. Niu, S. Bhattacharyya, E. A. Vitol, M. G. Schrlau, E. S. Papazoglou, G. Friedman, and Y. Gogotsi, "Multifunctional carbon-nanotube cellular endoscopes," *Nature Nanotechnology* 6:57-64, 2011.

[14]J. J. Niu, M. G. Schrlau, G. Friedman, and Y. Gogotsi, "Carbon nanotube-tipped endoscope for in situ intracellular surface-enhanced Raman spectroscopy," *Small*, 7:540-545, 2011.

[15]X. Chi, D. Huang, Z. Zhao, Z. Zhou, Z. Yin, and J. Gao, "Nanoprobes for in vitro diagnostics of cancer and infectious diseases," *Biomaterials*, 33:189-206, 2012.

[16]M. G. Schrlau, E. M. Falls, B. L. Zieber, and H. H. Bau, "Carbon nanopipettes for cell probes and intracellular injection," *Nanotechnology*, 19:015101 (4 pp.), 2008.

[17]M. Golshadi and M. G. Schrlau, "Template-Based Synthesis of Aligned Carbon Nanotube Arrays for Microfluidic and Nanofluidic Applications," *ECS Transactions*, 50:1-14, 2013.

[18]J. R. Freedman, D. Mattia, G. Korneva, Y. Gogotsi, G. Friedman, and A. K. Fontecchio, "Magnetically assembled carbon nanotube tipped pipettes," *Applied Physics Letters*, 75:103108 (3 pp.), 2007.

[19]R. Singhal, S. Bhattacharyya, Z. Orynbayeva, E. Vitol, G. Friedman, and Y. Gogotsi, "Small diameter carbon nanopipettes," *Nanotechnology*, 21:015304 (9 pp.), 2010.

[20]"P-2000 Laser Based Micropipette Puller System Operation Manual," ed: Sutter Instruments Company, 2010.

[21]M. Golshadi, J. Maita, D. Lanza, M. Zeiger, V. Presser, and M. G. Schrlau, "Effects of synthesis parameters on carbon nanotubes manufactured by template-based chemical vapor deposition," *Carbon*, 80:28-39, 2014.

[22]D. Ogden, "Microelectrode techniques: the Plymouth Workshop handbook," ed: Company of Biologists Limited, 1994.